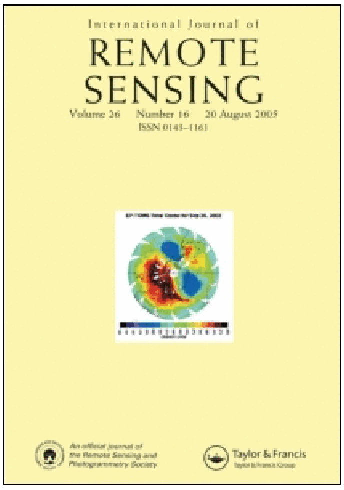

International Journal of Remote Sensing
Publication details, including instructions for authors and subscription information:
http://www.informaworld.com/smpp/title~content=t713722504

Geometric accuracy assessment of the orthorectification process from very high resolution satellite imagery for Common Agricultural Policy purposes

M. A. Aguilar [a]; F. Agüera [a]; F. J. Aguilar [a]; F. Carvajal [a]
[a] Departamento de Ingeniería Rural, University of Almería, Escuela Politécnica Superior, 04120 Almería, Spain

Online Publication Date: 01 December 2008

To cite this Article Aguilar, M. A., Agüera, F., Aguilar, F. J. and Carvajal, F.(2008)'Geometric accuracy assessment of the orthorectification process from very high resolution satellite imagery for Common Agricultural Policy purposes',International Journal of Remote Sensing,29:24,7181 — 7197

To link to this Article: DOI: 10.1080/01431160802238393

URL: http://dx.doi.org/10.1080/01431160802238393

International Journal of Remote Sensing
Vol. 29, No. 24, 20 December 2008, 7181–7197

Geometric accuracy assessment of the orthorectification process from very high resolution satellite imagery for Common Agricultural Policy purposes

M. A. AGUILAR*, F. AGÜERA, F. J. AGUILAR and F. CARVAJAL
Departamento de Ingeniería Rural, University of Almería, Escuela Politécnica Superior, La Cañada, 04120 Almería, Spain

(*Received 10 January 2007; in final form 23 March 2008*)

This study has, as its main aim, the assessment of different sensor models to achieve the best geometric accuracy in orthorectified imagery products obtained from IKONOS Geo Ortho Kit and QuickBird basic imagery. The final orthoimages are compared, both geometrically and visually, with the panchromatic orthophotos based on a photogrammetric flight with an approximate scale of 1 : 20 000, which are now used for the European Union Common Agricultural Policy in Andalusia (Spain). Two-dimensional root mean square (RMS_{2d}) errors in independent check points are used as accuracy indicators. The ancillary data were generated by high accuracy methods: (1) check and ground control points (GCPs) were measured with a differential global positioning system and (2) an accurate digital elevation model was used for image orthorectification. Two sensor models were used to correct the satellite data: (1) a three-dimensional (3D) rational function refined by the user with zero- (RPC0) or first-(RPC1) order polynomial adjustment and (2) the 3D Toutin physical model (CCRS). For the IKONOS image, the best results in the final orthoimages (RMS_{2d} of about 1.15 m) were obtained when the RPC0 model was used. Neither a large number of GCPs (more than nine), nor a better distribution of them, improved the results obtained with the RPC0. For the QuickBird image, the CCRS model generated the best results (RMS_{2d} of about 1.04 m), although it was sensitive to the number and distribution of the GCPs used in its computation.

1. Introduction

With the launch of the first two very high resolution (VHR) satellites, IKONOS in September 1999, with 1 m as the nominal ground sample distance (GSD), and QuickBird in October 2001, with 0.61 m as the nominal GSD, conventional aerial photogrammetric mapping at large scales began to have serious competitors (Fraser 2002, Kay *et al*. 2003, Chmiel *et al*. 2004). In June 2003, OrbView-3 was added to satellites with a nominal GSD of 1 m. In addition, several high resolution (0.7 to 1 m GSD) optical space systems, such as EROS B1, Resource-DK-1 and KOMPSAT-2, were also launched during 2006. Another new satellite called WorldView-1, launched in September 2007, can obtain panchromatic images with 0.5 m resolution imagery. A higher resolution will be made available by WorldView-2 and GeoEye-1. The rapid increase of VHR satellite sensors in the next few years will result in improvements in resolution, availability and cost.

*Corresponding author. Email: maguilar@ual.es

International Journal of Remote Sensing
ISSN 0143-1161 print/ISSN 1366-5901 online © 2008 Taylor & Francis
http://www.tandf.co.uk/journals
DOI: 10.1080/01431160802238393

Mapping agencies became interested in the potential of the IKONOS and QuickBird sensors in 1996, long before they were eventually launched (Ridley *et al.* 1997). The mapping agency of Great Britain, Ordnance Survey, has carried out several research projects to study the main potential uses of VHR satellite imagery: change detection (i.e. merely detecting that a change has occurred), topographic map update (i.e. measuring and capturing the change in a spatial database), map currency auditing (independently checking the currency of the spatial database) and land cover mapping (Holland *et al.* 2006).

Much research work has been carried out in the last years to study the influence of the number and distribution of ground control points (GCPs) on the geometric accuracy reached in the final IKONOS and QuickBird corrected panchromatic image using different sensor models (Zhou and Li 2000, Davis and Wang 2003, Kay *et al.* 2003, Wolniewicz 2004, Fraser and Hanley 2005, Shaker *et al.* 2005, Wang and Ellis 2005, Fraser *et al.* 2006). As a summary, Toutin (2004) reported, in his review article, that the number of GCPs required for satellite imagery correction was derived from a function of different conditions: collection method, sensor type and resolution, image spacing, geometric model, study site, physical environment, GCPs definition and accuracy and final expected accuracy.

Bearing in mind that in the European Union countries, agricultural policies have culminated in official requirements for the obligatory use of techniques to control subsidy payments, preferably based on very accurate orthoimages (EUR-Lex 2000), and that these orthophotos can be obtained from VHR satellite data (Kay *et al.* 2003, Chmiel *et al.* 2004, Rossi and Volpe 2005), the geometrical accuracy assessment of the orthorectification process from VHR satellite imagery is acquiring great importance. In fact, the Andalusian Government (Spain) recently made available for public viewing a panchromatic orthophoto with a 0.5 m GSD covering all its territory, based on a photogrammetric flight with an approximate scale of 1 : 20 000, taken during 2001 and 2002 (Andalusian Government 2004). This product has been used, among others, for the European Union Common Agricultural Policy. In addition, according to the technical requirements and recommendations defined by the Joint Research Centre (Kay 2002), a Directorate General of the European Commission, an orthophoto must not be older than 5 years. Therefore, it must be in constant renovation.

The necessary steps and the ancillary data to update or generate orthoimages from raw VHR satellite imagery have already been studied in a previous work (Aguilar *et al.* 2007a), where the aim was to study the different methodological approaches to achieve the best possible geometric accuracy in orthorectified imagery products obtained from panchromatic QuickBird basic imagery in an operational environment.

The current paper continues the research carried out by Aguilar *et al.* (2007a) on the geometric accuracy issues of panchromatic VHR satellite imagery orthorectification. The influence that factors, such as the number and distribution of GCPs and the sensor model used for the geometric corrections of the satellite image, have on the geometric accuracy obtained in the sensor orientation phase and in the final orthoimage has been evaluated over an IKONOS Geo Ortho Kit and a QuickBird basic image. The final orthoimages obtained from IKONOS and QuickBird will be compared, both geometrically and visually, with the panchromatic orthophotos that are now used for the European Union Common Agricultural Policy in Andalusia (Spain). The principal innovation with regard to other works published previously, in addition to the high number of used repetitions, is that the products obtained for QuickBird and IKONOS have been generated in the same operational conditions: the same study area, the same ground points and the same digital elevation model (DEM).

2. Study site and dataset

2.1 *Study site*

The study site is an area situated to the north-east of the city of Almería, Spain, specifically in the region of Campo de Níjar (figure 1). It is a zone occupied principally by greenhouses, with rather flat relief, although there are some mountain ranges. Figure 2 shows the DEM of the study area on the European Datum ED50 with the International Ellipsoid from Hayford and projection to the UTM 30 N. The area covered by the IKONOS scene (rectangle with black line) has an elevation range of between 45 to 361 m above sea level, whereas the zone covered by the QuickBird scene (rectangle with white line) ranges from 45 to 850 m.

2.2 *The IKONOS Geo Ortho Kit image*

In September 2005, we acquired from European Space Imaging™, an archive image of the IKONOS Geo Ortho Kit, taken on 2 June 2005. The dimensions of this image were approximately 11 by 13 km and were centred on the European Datum ED50 coordinates (easting and northing) of 574 639 m and 4 083 543 m. Other characteristics of the IKONOS image are shown in table 1.

The IKONOS Geo Ortho Kit is the IKONOS commercial imagery format that presents the lowest level of corrections, both radiometric and geometric. Geo Ortho Kit images include the camera geometry obtained at the time of image collection. With the Geo Ortho Kit, users can produce their own highly accurate orthorectified products by utilizing commercial off-the-shelf software, DEMs and GCPs.

2.3 *The QuickBird basic image*

On 19 December 2004, a QuickBird panchromatic basic image was acquired. The basic scene was centred on the European Datum ED50 coordinates (easting and northing) of 577 901 and 4 087 237 m. Other characteristics of the basic image are shown in table 1.

Basic imagery is the least processed image product of the DigitalGlobe™ product suite. Only corrections for radiometric distortions and adjustments for internal

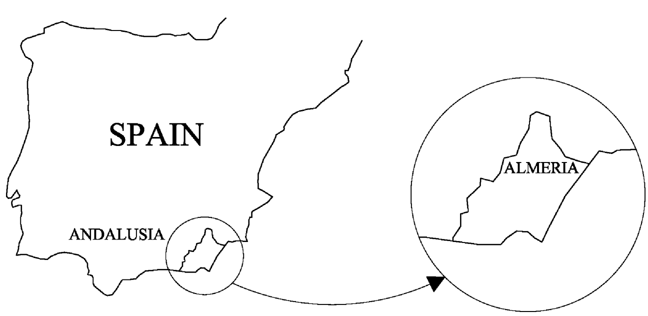

Figure 1. Location of the study area.

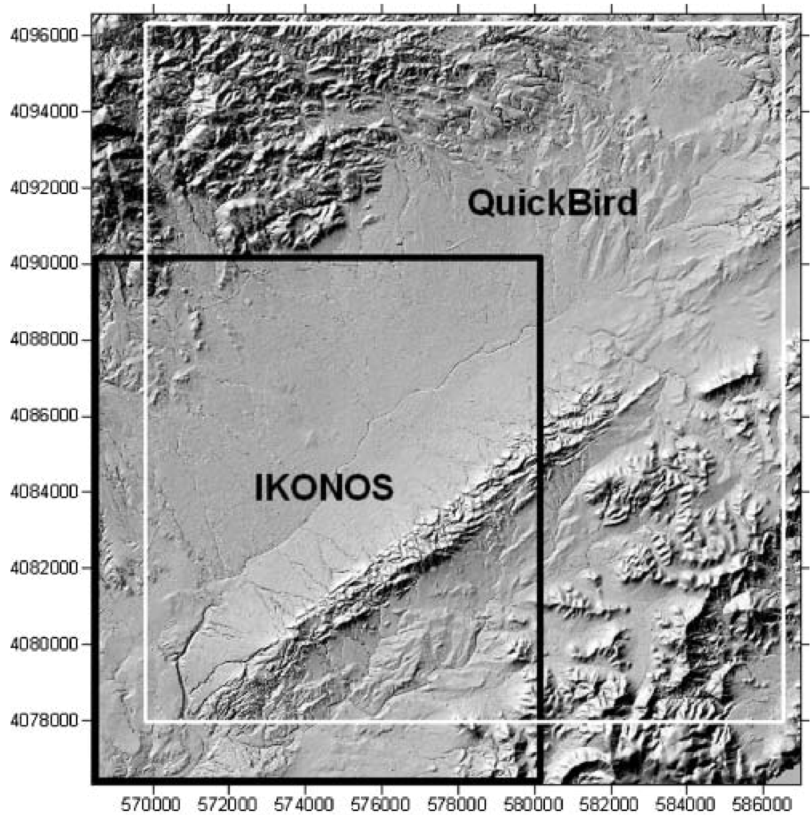

Figure 2. Digital elevation model of the study area covered by IKONOS and QuickBird imagery.

sensor geometry, optical and sensor distortions have been performed on each scene ordered. Basic imagery products are designed for users that have advanced image processing capabilities.

2.4 *Ground control and check points*

GCPs and independent check points (ICPs) were obtained using differential global positioning system (DGPS) receivers in both static and real-time kinematic (RTK) modes, with post-processing in both cases (Aguilar *et al.* 2007b). The goal was to

Table 1. Characteristics of the IKONOS and QuickBird panchromatic images used.

Product	IKONOS Geo Ortho Kit PAN	QuickBird basic image PAN
Acquisition date	02 June 2005	19 December 2004
Cloud cover	0%	6%
Sun angle azimuth	132.67°	163.0°
Sun angle elevation	70.22°	27.9°
Elevation angle	78.41°	80.9°
Collection azimuth	134.85°	123.3°
Acquired nominal GSD	0.84 m	0.62 m
Product pixel size	1 m	0.62 m

obtain a reliable measurement of ground points with accuracy better than a decimetre. Finally, the coordinates of the 251 points (GCPs and ICPs) distributed over full QuickBird and IKONOS scenes, referred to the ED 50 European Datum (Hayford International Ellipsoid), were collected using the UTM projection. The vertical datum adopted the geoid as reference surface. The ground points used in this study were well defined on the IKONOS (figure 3) and/or QuickBird (figure 4) images.

2.5 *Digital elevation model*

To generate panchromatic orthoimages from IKONOS and QuickBird, an accurate DEM was used. This DEM was obtained by the Andalusian Government from a panchromatic photogrammetric flight at an approximate scale of 1 : 20 000 realized in 2002. The Andalusian DEM was published in 2005 (Andalusian Government 2005). The original DEM in the study area, with a grid spacing of 10 m, was interpolated to 5 m using radial basis functions (Aguilar *et al*. 2005). Although it is not the aim of this paper, this resolution was used to compare the results with previous work on the same study site (Aguilar *et al*. 2007a), where we also used a medium DEM with a grid spacing of 5 m, which was derived by ourselves from digitized contour lines. The statistics of the differences of the 92 known DGPS

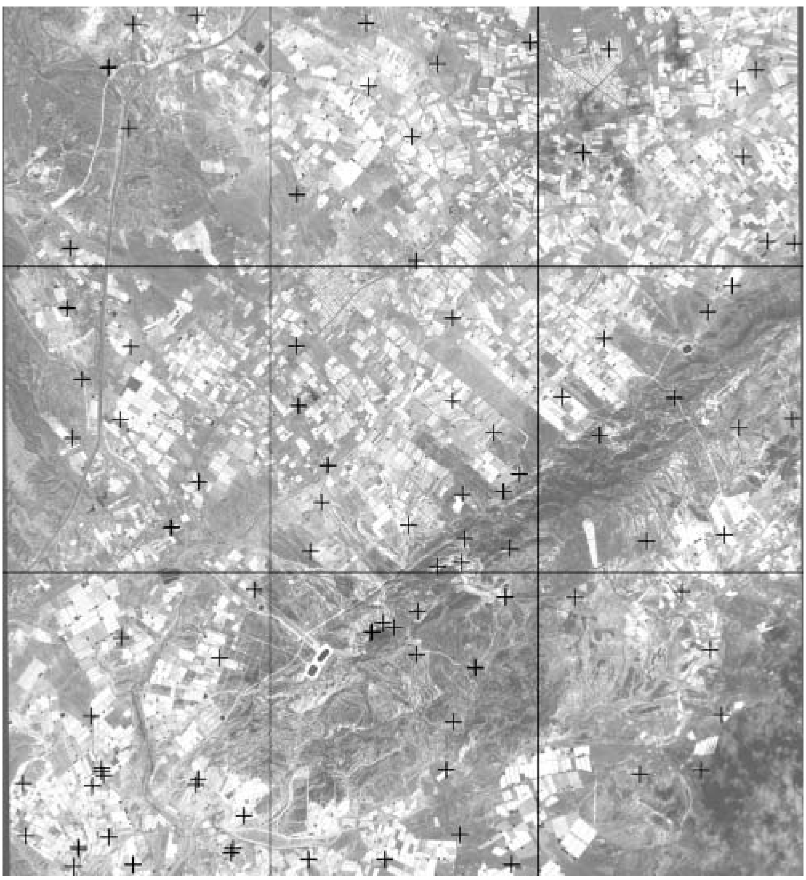

Figure 3. Distribution of 109 ground points (GCPs and ICPs) overlaid on the IKONOS Geo Ortho Kit panchromatic image.

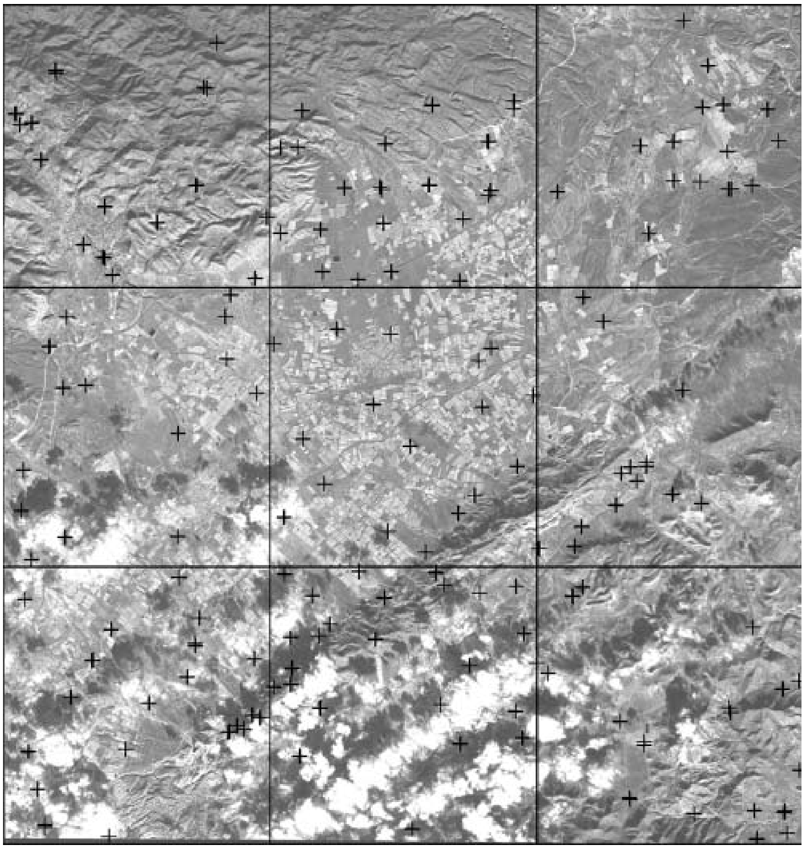

Figure 4. Distribution of 218 ground points (GCPs and ICPs) overlaid on the QuickBird basic panchromatic image.

coordinates, placed on the natural terrain in the area of interest, minus the DEM surface were as follows: mean error of −0.52 m, vertical root mean square error (RMSz) of 1.52 m and maximum error of 4.98 m.

3. Sensor models

A sensor model or geometric correction model is a mathematical equation that relates object point positions (X, Y, Z) to their corresponding two-dimensional (2D) image positions (x, y). The sensor models often used to correct satellite imagery can be separated into two categories: (1) generalized sensor models as 2D polynomial functions, three-dimensional (3D) polynomial functions, affine model and 3D rational functions (Tao and Hu 2001, Fraser and Yamakawa 2004, Fraser *et al.* 2006) and (2) physical models (Toutin 2004). Nevertheless, for VHR satellite images, two models are commonly used: (1) terrain-independent 3D rational functions with vendor image support data and (2) 3D physical models. These two models have been tested in this work and they are supported by OrthoEngine from PCI Geomatica v 9.1.7 (PCI Geomatics, Richmond Hill, Ontario, Canada), which is the commercial software we have used. A summarized relation of the sensor models used in this work is carried out below. A more detailed description of them can be found in Aguilar *et al.* (2007a).

3.1 *Terrain-independent 3D rational functions with vendor image support data*

Third-order rational polynomial coefficients (RPCs) are usually distributed by the image vendor in VHR sensors, such as IKONOS or QuickBird. Nevertheless, the users can update or improve the accuracy of the rational function model using a few GCPs. The refining method most used is based on added complementary transformation (usually polynomial) in image or object space, so the original RPCs remain constant. The OrthoEngine RPC refining method is based on the block adjustment method developed by Grodecki and Dial (2003) for image space.

In most cases, a zero-order polynomial adjustment is adequate for IKONOS images (RPC0) and at least one GCP is necessary to compute both parameters; however, for QuickBird images, a first-order polynomial adjustment (RPC1) is required to achieve the best results. In this case, it is necessary to know at least three GCPs. The 9.1.7 of the PCI Geomatica version supports both zero- (RPC0) and first- (RPC1) order polynomial adjustment (Cheng *et al.* 2005), which have been tested in this work.

In general, the RPCs can be treacherous for the potential user because the process can be too automatic, especially if GCPs to refine the solution are not used. If, for example, there is an error in the RPCs that the vendor is providing with the imagery, then the user could have difficulty in discovering it because the user has little or no control of these coefficients.

3.2 *The 3D physical model*

A 3D physical model developed by Toutin (Toutin and Cheng 2002, Toutin 2003) at the Canada Centre for Remote Sensing (CCRS) is also tested in this study for the IKONOS and QuickBird imagery.

4. Methodology

4.1 *Studied cases*

In an orthoimage, the 2D geometric error can be expressed as the sum of the error in the bundle adjustment phase (also known as sensor orientation phase or triangulation) and the 2D orthoimage error propagated from the DEM error. These terms are expressed as root mean square error (RMS) in this work.

Thus, we have studied separately the errors in the orientation or bundle adjustment phase and in the final orthoimage in three different cases:

(1) Computing the sensor models for the QuickBird image with GCPs spread over the full QuickBird scene. In this case, 218 ground points were used (figure 4). We refer to this case as QB-I.
(2) Obtaining the sensor orientations for the IKONOS image from GCPs distributed along the full IKONOS scene. In this case, 109 ground points were used (figure 3). We refer to this case as IKONOS.
(3) Performing the bundle adjustment for the QuickBird image using only ground points located inside the overlap area of QuickBird and IKONOS scenes. In this case, 104 ground points were used. We refer to this case as QB-II.

4.2 *Sensor orientation phase*

The aim of this test was to observe the two-dimensional root mean square error (RMS_{2d}) in the sensor orientation phase depending on, first, the number and distribution of the GCPs that take part in the bundle adjustment, second, the sensor model used and third, the cases studied (QB-I, QB-II and IKONOS). For every case, 15 repetitions of 9 and 18 GCPs, respectively, were extracted from the initial ground points. The samplings were carried out in two different ways: (1) completely random sampling and (2) stratified random sampling. For the latter type of sampling, the different case scenes were divided into nine equal sub-areas, e.g. for IKONOS and QB-I cases, see figures 3 and 4, respectively. To generate the repetitions of 9 and 18 GCPs with stratified random sampling, one or two GCPs were chosen in each of the sub-areas mentioned above. Therefore, a total of 60 sets of GCPs were extracted for each one of the cases studied. In general, the GCPs spatial distribution in the combinations carried out according to a completely random sampling was worse than those carried out by means of stratified random sampling.

Thus, 180 photogrammetric projects were computed for every studied case (60 sets of GCPs and three sensor models). The RMS_{2d} in the rest of the ground points (100 or 91 ICPs for IKONOS, 209 or 200 for QB-I and 95 or 86 for QB-II, respectively) was computed for every project. The RMS_{2d} was calculated for each photogrammetric project using the ICP datasets by

$$RMS_{2d} = \sqrt{RMS_x^2 + RMS_y^2}, \qquad (1)$$

where RMS_x and RMS_y are the RMS errors in the x and y directions, respectively.

Some statistics of the RMS_{2d} (mean, standard deviation, maximum and minimum value) were estimated from 15 repetitions over both types of samplings and the number of GCPs.

4.3 *Image orthorectification phase*

With this second test, we wanted to know the geometric accuracy that we finally obtained in the orthorectified images, using the previously described DEM. This accuracy (RMS_{2d}) was calculated over the same 80 ICPs that were well defined and homogeneously distributed on the IKONOS and QuickBird scenes. Therefore, they were placed on the overlap of both scenes. The ground coordinates of the ICPs in this phase were extracted from a vectorial cartography at a scale of 1 : 1000 that was generated in 2002 by our research group by order of the Council of Agriculture of the Andalusian Government. Most of these points were corners of greenhouses that can be very well pointed in both satellite images. The 80 ICPs were also well defined on the Andalusian Government's orthophoto based on a photogrammetric flight.

To decrease the number of orthophotos checked, and due to the great geometric accuracy required for the final products, all the orthoimages generated in this work were computed using 18 GCPs selected by stratified random sampling. Of the 15 repetitions generated in the sensor orientation phase, for each of the three studied cases (QB-I, QB-II and IKONOS) and for every sensor model, only six were selected to generate orthoimages. Thus, 54 orthoimages were computed in this work (six repetitions, three sensor models and three cases studied). For every case, the aim was to select six repetitions that were representing all the ones generated in the previous section. Thus, the RMS_{2d} statistics (mean and standard deviation) calculated for the six selected combinations in the orientation phase were practically identical to the ones obtained for the 15 original repetitions.

The digital orthophotos created had 0.6 m and 1 m GSD for QuickBird (QB-I and QB-II) and IKONOS, respectively. The sinusoidal resampling kernel ($\sin(x)/x$ with

16×16 windows) was the resampling method used for the radiometric operation carried out in all the orthorectified images generated in this work.

5. Results and discussion

5.1 *Sensor orientation phase*

In table 2, the RMS_{2d} statistics in the sensor orientation phase for the 15 repetitions generated for each of the sensor models, number of GCPs and type of sampling studied for the full IKONOS scene are shown. When the number of GCPs was small and they presented a bad distribution (nine GCPs chosen by random sampling), the CCRS showed the worst results, with RMS_{2d} mean value of 2.09 m and a very high standard deviation (Sd). The RMS_{2d} statistics obtained by the CCRS improved considerably when the number of GCPs increased or when they were better distributed.

The poor results obtained by the CCRS for the IKONOS case were due to the fact that detailed sensor/satellite information for IKONOS is not released by Space Imaging. Thus, it is difficult to develop a parametric sensor model that reflects the physical reality of the complete viewing geometry for the IKONOS sensor (Tao *et al*. 2004). As we can see later, the results generated with this sensor model were greatly improved for QuickBird basic images, as the information given by DigitalGlobe on their sensor is very complete.

For the IKONOS image, sensor models that use the RPCs supplied by the vendor (RPC0 and RPC1) provided the best results and were much more independent from the number and situation of the GCPs used than the CCRS. This was especially true for the RPC0, where an RMS_{2d} very close to 0.60 m was obtained in any of the 60 combinations used in this work. The results confirmed previous experiments (Fraser and Hanley 2005, Toutin 2006) that a shift (RPC0) was enough to improve supplied RPCs of IKONOS. The RPC1 model did not improve the results from the RPC0; in addition, both the number and location of the GCPs was important (Fraser and Hanley 2005).

In table 3, the RMS_{2d} statistics in the sensor orientation phase for the QB-I case are shown. Here, the best geometric accuracies were obtained when the CCRS

Table 2. RMS_{2d} statistics for the 15 repetitions obtained in the sensor orientation phase for the full IKONOS scene.

		Random sampling		Stratified random sampling	
Sensor models	Statistics	9 GCPs	18 GCPs	9 GCPs	18 GCPs
CCRS	Mean (m)	2.09	1.07	1.09	0.94
	Sd (m)	1.40	0.22	0.23	0.07
	Maximum (m)	5.59	1.56	1.78	1.06
	Minimum (m)	0.98	0.85	0.76	0.80
RPC0	Mean (m)	0.60	0.57	0.60	0.59
	Sd (m)	0.03	0.02	0.04	0.03
	Maximum (m)	0.69	0.60	0.70	0.64
	Minimum (m)	0.56	0.55	0.56	0.55
RPC1	Mean (m)	0.82	0.59	0.63	0.59
	Sd (m)	0.28	0.04	0.07	0.04
	Maximum (m)	1.40	0.68	0.75	0.70
	Minimum (m)	0.55	0.54	0.55	0.55

Table 3. RMS_{2d} statistics for the 15 repetitions obtained in the sensor orientation phase for the full QuickBird scene (QB-I).

		Random sampling		Stratified random sampling	
Sensor models	Statistics	9 GCPs	18 GCPs	9 GCPs	18 GCPs
CCRS	Mean (m)	1.81	1.08	1.21	0.95
	Sd (m)	1.35	0.23	0.36	0.12
	Maximum (m)	6.40	1.73	1.79	1.20
	Minimum (m)	0.96	0.89	0.82	0.80
RPC0	Mean (m)	1.74	1.67	1.71	1.66
	Sd (m)	0.07	0.04	0.05	0.02
	Maximum (m)	1.87	1.76	1.85	1.71
	Minimum (m)	1.64	1.62	1.66	1.63
RPC1	Mean (m)	1.95	1.15	1.56	1.07
	Sd (m)	0.64	0.29	0.42	0.12
	Maximum (m)	3.54	1.85	2.28	1.38
	Minimum (m)	1.23	0.87	1.05	0.89

sensor models were used with 18 GCPs chosen by stratified random sampling. This sensor model was again very dependent on the number and the distribution of the GCPs used in their computation. In fact, Wolniewicz (2004) has already reported that the CCRS approach was very sensitive in accuracy for the distribution of the GCPs in a range from 7 to 10.

Among the sensor models that use the vendor's RPCs, the RPC1 obtained better results in the QuickBird basic image, as reported by several researchers (e.g. Niu *et al*. 2004, Fraser *et al*. 2006). Although the RPC0 sensor model continued being stable, as in the previous case, the computed RMS_{2d} was now always close to 1.70 m, a much higher value than the original GSD.

When the geometric accuracy was studied in the orientation phase for QB-II (table 4), the RMS_{2d} computed by the CCRS decreased with regard to the ones shown in table 3 for QB-I. This could be due to the fact that the terrain relief was much flatter in the QB-II case, since the ground points placed on the Alhamilla mountain range, to the north-west of the QuickBird scene and on the Gata

Table 4. RMS_{2d} statistics for the 15 repetitions obtained in the sensor orientation phase for the split QuickBird scene (QB-II).

		Random sampling		Stratified random sampling	
Sensor models	Statistics	9 GCPs	18 GCPs	9 GCPs	18 GCPs
CCRS	Mean (m)	1.36	0.75	0.92	0.73
	Sd (m)	0.53	0.09	0.16	0.12
	Maximum (m)	2.40	0.95	1.28	1.02
	Minimum (m)	0.77	0.62	0.70	0.58
RPC0	Mean (m)	1.15	1.01	1.09	0.99
	Sd (m)	0.07	0.04	0.08	0.06
	Maximum (m)	1.32	1.06	1.20	1.07
	Minimum (m)	1.05	0.93	0.89	0.88
RPC1	Mean (m)	2.20	1.25	1.54	1.06
	Sd (m)	0.53	0.22	0.31	0.13
	Maximum (m)	3.20	1.71	2.19	1.38
	Minimum (m)	1.26	0.97	0.73	0.93

mountain range to the south-east (figure 2) were suppressed. The terrain relief index computed as the standard deviation of the height of the 218 ground points took a value of 115 m for the QB-I case and 50 m for the QB-II case, computed at 104 ground points. Both values were very high compared with those reported by Wang and Ellis (2005), which ranged from 28.8 m in hilly terrain to 1.8 m in flat terrain. It is necessary to bear in mind that terrain relief can affect the accuracy of the corrected image, as already reported for IKONOS imagery by Toutin (2003) and Wang and Ellis (2005).

Although the CCRS is a rigorous model, it depends on the location of the GCPs. Thus, the GCPs must be well distributed in planimetry and cover the full elevation range of the terrain. In figure 5, the variation of RMS_{2d} with the elevation range of the GCPs used to generate the bundle adjustment in the case QB-I for the CCRS is shown. For this figure, 30 sets of 9 GCPs chosen by stratified random sampling were used. The RMS_{2d} values decreased (coefficient of determination, $r^2>0.63$) when the selected GCPs covered a higher elevation range. Due to this, the best results obtained from the QuickBird basic image (QB-I and QB-II) were produced when 18 GCPs chosen by stratified sampling were used. In this case, the GCPs were spread both in planimetry and in altimetry (lowest and highest elevations).

The results obtained with the RPC1 sensor model were very similar in cases QB-I and QB-II. Nevertheless, the RMS_{2d} values generated on ICPs in all the 60 GCP combinations studied improved from about 1.70 m for QB-I to 1 m for QB-II when the RPC0 was used. The RPC0 provoked systematic errors for QuickBird images that increased with the distance to the centre of the scene. These types of error distributions have already been reported by Noguchi *et al.* (2004), Fraser and Hanley (2005) and Aguilar *et al.* (2007a). In figure 6, the radial residual systematic errors, mainly in the along-track direction, which were not being modelled by the RPC0 are shown. Since these errors were proportional to the distance to the centre of the image, they were smaller in QB-II, as the area was smaller in this case than in QB-I. These systematic errors were not observed in the IKONOS case with the RPC0.

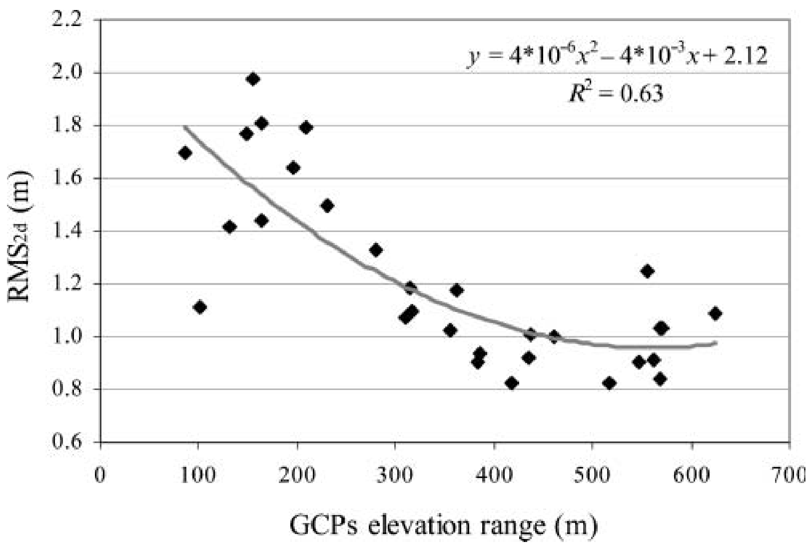

Figure 5. Relation between the elevation range of the GCPs used to compute the bundle adjustment and the RMS_{2d} obtained at the ICPs.

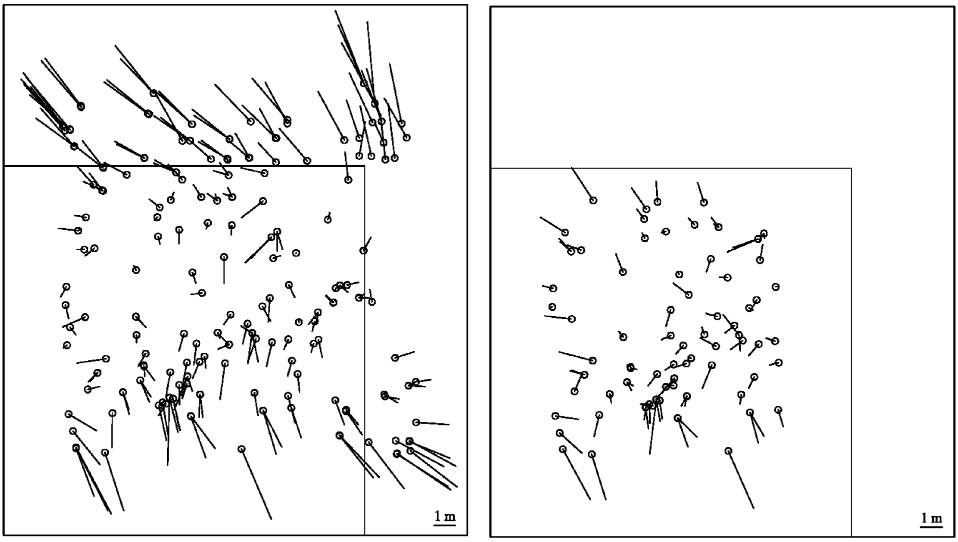

(*a*) (*b*)

Figure 6. Ground coordinates residuals distribution for 18 GCPs and stratified random sampling in the orientation phase: (*a*) RPC0 for a full scene of QuickBird and (*b*) RPC0 for a split QuickBird scene.

The improvement of the results generated by the RPC0 for QB-II also might be related to the flattest relief presented in this case. In fact, Toutin (2006) suggested that the QuickBird RPC model is relief dependent, i.e. the stronger the relief, the larger the polynomial order should be to refine the RPCs.

5.2 *Image orthorectification phase*

The second test was carried out to verify the final geometric accuracy obtained over IKONOS and QuickBird (QB-I and QB-II) orthoimages, i.e. in the final product of the orthorectification process. In figure 7, the mean values and error bars representing the 95% confidence interval (1.96σ) obtained for RMS_{2d} at 80 ICPs are shown. For the orthoimages generated from the QuickBird basic image, the best geometric accuracies were obtained using the CCRS sensor model, both for case QB-I and QB-II. The RMS_{2d} mean values were about 1.04 m, although when the CCRS model was used with case QB-I the mean RMS_{2d} reached 1.11 m. As a rule, the confidence intervals of RMS_{2d} were placed between 1 m and 1.15 m for the CCRS. When calculating the CCRS sensor model with GCPs placed exclusively in the area of interest (QB-II), better results were obtained than when they were distributed over the whole scene (QB-I). When the RPC0 or RPC1 were used for the orthorectification of QuickBird imagery, the 95% confidence intervals range from 1.17 m up to 1.45 m.

On the other hand, the best results for the orthoimages computed from the IKONOS Geo Ortho Kit image were obtained using the sensor models that employ the RPCs supplied by the vendor. Mean values of RMS_{2d} of 1.15 m and 1.12 m were generated by the RPC0 and RPC1, respectively. Moreover, the confidence intervals obtained with these sensor models were much reduced, i.e. the reliability reached for the computed RMS_{2d} is very high. Higher mean values of RMS_{2d} (1.34 m) and longer confidence intervals were generated by the CCRS sensor model.

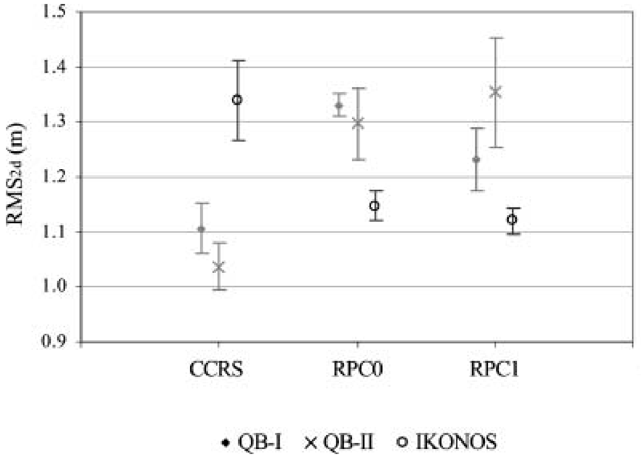

Figure 7. Mean values and error bars represent the 95% confidence interval for the two-dimensional RMS at 80 ICPs, obtained for six repetitions over orthoimages from QuickBird and IKONOS.

Researchers have obtained very heterogeneous results for the geometric accuracy in QuickBird or IKONOS panchromatic orthoimages. This is fundamentally due to the great variety of ancillary data (GCPs and DEM), sensor models, terrain relief and, to a lesser extent, the different satellite view angle employed (Chmiel *et al.* 2004). For flat areas, using a 5 to 7 m accuracy DEM and with DGPS GCPs, Wolniewicz (2004) obtained IKONOS and QuickBird orthoimages with RMS_{2d} values of about 1.23 m and 1.13 m, respectively. For a mountain area, RMS_{2d} values of around of 1.58 m for orthophotos from both sensors were obtained. With a similar DEM (RMS_z<5 m) and GCPs, Kay *et al.* (2003) generated IKONOS orthorectified images with a RMS_{2d} of around 2 m and QuickBird orthoimages with a RMS_{2d} of 1.54 m. On the other hand, Davis and Wang (2003) reported a RMS_{2d} of around 1 m measured in IKONOS orthoimages located in an urban area of Springfield, MO, using 2 m accuracy DEM.

The Andalusian Government in Spain is very interested in creating and updating orthoimages across the whole area of Andalusia in order to use them for a variety of purposes, amongst which the European Union Common Agricultural Policy is paramount. In fact, in order to administrate and control farmers' declarations, the European Union created an Integrated Administration and Control System (IACS) in 1992. In a second step, obliged by the 1593/2000 Council Regulation (EUR-Lex 2000), the declaration process was improved by the establishment of a land parcel identification system based on orthoimages with a homogenous standard guaranteeing a level of accuracy equivalent at least to a cartography a scale of 1 : 10 000. Thus, these orthoimages should have a pixel size smaller than 1 m and one-dimensional RMS (RMS_{1d}) lower than 2.5 m (Kay 2002). Due to this, the Andalusian Government recently made available for public viewing a panchromatic orthophoto with a 0.5 m GSD based on a photogrammetric flight. The RMS_{2d} of this product was computed in the same 80 ICPs used in this study, obtaining a value of 1.46 m. Better RMS_{2d} results were obtained with IKONOS or QuickBird orthoimages in this work.

In figure 8, orthoimages from IKONOS, QuickBird and photogrammetric flight are compared visually on the same area. All the orthophotos in figure 8 have been generated as 8 bit images, although the original scenes of QuickBird and IKONOS are 11 bit, which could improve feature classification and identification in dark or bright areas. In the case of figure 8, the QuickBird orthoimages subjectively present the best visual quality. However, we must bear in mind that factors such as the lighting or the season in which the images were captured could be the reasons for these visual differences, e.g. the atmosphere can be clear in December especially after rainfall (the QuickBird basic image was taken in this season), while it can be

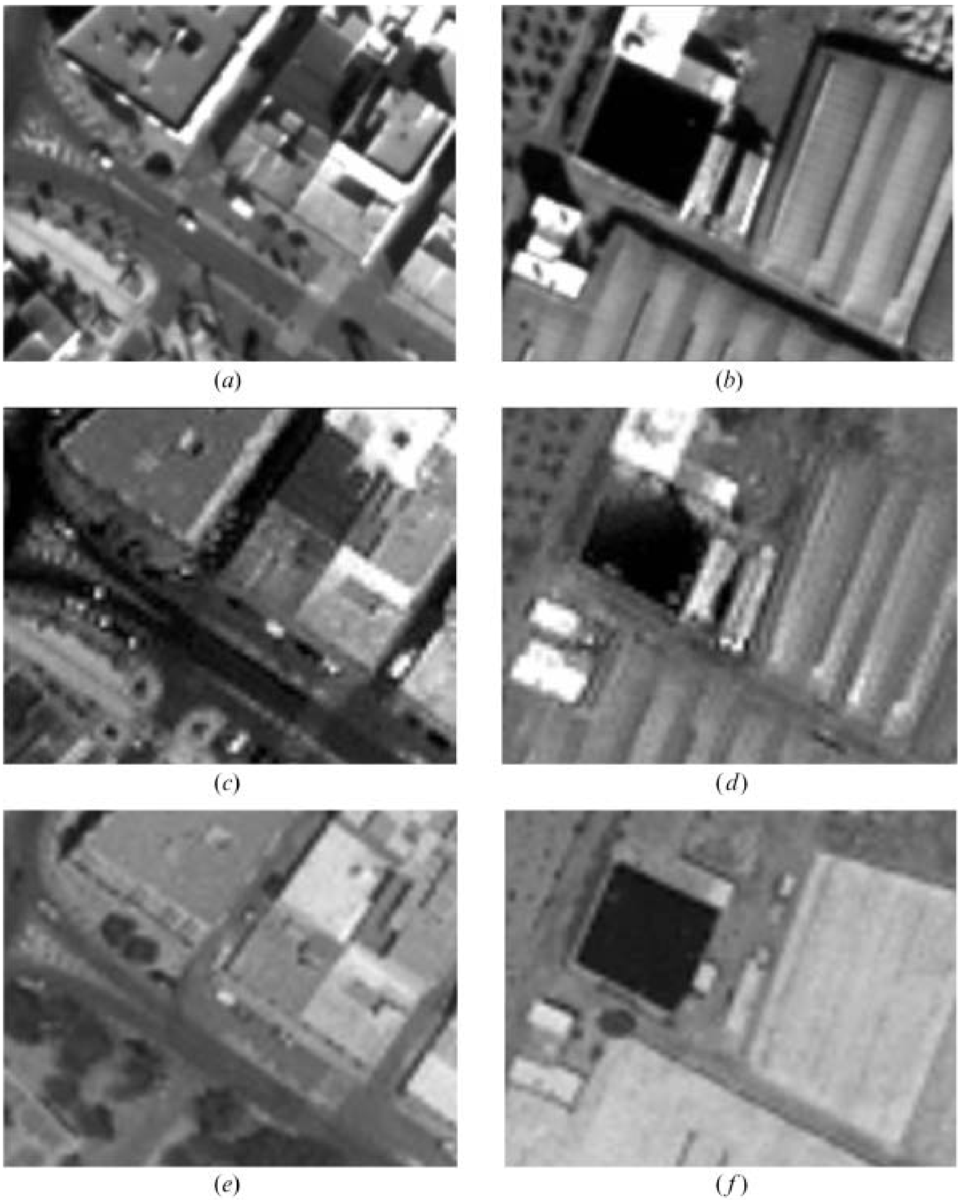

Figure 8. Orthoimages (72 m per 68 m) obtained at the study site from: (*a*) and (*b*) QuickBird with 0.6 m GSD, (*c*) and (*d*) IKONOS with 1 m GSD and (*e*) and (*f*) photogrammetric flight at an approximate scale of 1 : 20 000 with 0.5 m GSD.

hazy in June or July (when IKONOS and photogrammetric flight images were taken) due to dust or smog.

If the users employ IKONOS or QuickBird images with a small off-nadir, good quality DEM (RMSz<2.5 m) and ground points measured with DGPS, they can reach the specifications for the orthoimages proposed by the European Union with any of the sensor models and combinations of GCPs tested in this work. In operational conditions and obviating the economic topic, our recommendation is to generate orthophotos from QuickBird basic images using the CCRS and 18 GCPs that are very well distributed, both horizontally and vertically, in the study area.

The generation of accurate orthoimages from VHR satellite imagery is the first step for the later application of techniques for detecting changes in land use or land cover use. At the study site, the greenhouse changes were detected directly when the results of the classification from a QuickBird's orthoimage were compared with a previous digital cartography (Agüera *et al.* 2006).

6. Conclusions

The best results in the sensor orientation phase for the IKONOS Geo Ortho Kit image were obtained when the RPC0 model was used. The RMS_{2d} for sensor orientation was around 0.60 m for all the cases studied and computed by this mathematical approach. With the RPC0, the number and distribution of the GCPs used did not influence the results, and very small values were obtained for standard deviation (about 0.03 m). For the QuickBird basic image, the CCRS generated the best results in the orientation phase, although this sensor model showed a great sensibility to the number and distribution of GCPs in all the cases studied.

With regard to the orthorectified IKONOS images, the best RMS_{2d} mean values were of 1.15 m and 1.12 m for the RPC0 and RPC1 respectively. Besides, the reliability reached for the computed RMS_{2d} is very high with these sensor models. Nevertheless, the CCRS was the sensor model that generated the most accurate orthoimages from QuickBird basic imagery, both for cases QB-I and QB-II (RMS_{2d} mean values less than 1.11 m). Better results were obtained when calculating the CCRS with GCPs placed exclusively in the area of interest (QB-II) than when they were distributed over the whole scene (QB-I).

The orthoimages generated from QuickBird and IKONOS had a geometric accuracy higher than the orthoimages obtained by the Andalusian Government from a photogrammetric flight for the European Union Common Agricultural Policy; in addition, the QuickBird orthophotos subjectively presented the best visual quality. Thus, when panchromatic QuickBird basic imagery are used to generate orthoimages in operational conditions, at least 18 GCPs should be chosen along the area of interest with stratified random sampling and the CCRS sensor model should be used. Even if the distribution of the GCPs is the best possible, both horizontally and vertically, it is likely that the number of GCPs needed to obtain a high level of reliability in the geometric accuracy of the orthoimages may be lower than 18.

Acknowledgements

The authors are grateful to the Public Enterprise for Agriculture and Fishery of Andalusia (D.a.p.) for their collaboration in the preparation of this study. This research work has been financed by the project 'Generation, integration and update of digital cartography as a support for rural sustainable development. Methodology and application in Campo de Níjar (Almería)' subsidised by the Andalusian Government.

References

AGÜERA, F., AGUILAR, M.A. and AGUILAR, F.J., 2006, Detecting greenhouse changes from QuickBird imagery on the Mediterranean coast. *International Journal of Remote Sensing*, **27**, pp. 4751–4767.

AGUILAR, F.J., AGÜERA, F., AGUILAR, M.A. and CARVAJAL, F., 2005, Effects of terrain morphology, sampling density, and interpolation methods on grid DEM Accuracy. *Photogrammetric Engineering and Remote Sensing*, **71**, pp. 805–816.

AGUILAR, M.A., AGUILAR, F.J., AGÜERA, F. and SÁNCHEZ, J.A., 2007a, Geometric accuracy assessment of QuickBird basic imagery using different operational approaches. *Photogrammetric Engineering and Remote Sensing*, **73**, pp. 1321–1332.

AGUILAR, F.J., CARVAJAL, F., AGUILAR, M.A. and AGÜERA, F., 2007b, Developing digital cartography in rural planning applications. *Computers and Electronics in Agriculture*, **55**, pp. 89–106.

ANDALUSIAN GOVERNMENT 2004, *Ortofotografía Digital de Andalucía*, Junta de Andalucía, Sevilla, Spain (on DVD).

ANDALUSIAN GOVERNMENT 2005, *Modelo Digital del Terreno de Andalucía. Relieve y orografía*, Junta de Andalucía, Sevilla, Spain (on DVD).

CHENG, P., SMITH, D. and SUTTON, S., 2005, Mapping of QuickBird images using the RPC method improvement in accuracy since release of first QuickBird data. *GEOInformatics*, **8**, pp. 50–52.

CHMIEL, J., KAY, S. and SPRUYT, P., 2004, Orthorectification and geometric quality assessment of very high spatial resolution satellite imagery for Common Agricultural Policy purposes. In *Proceedings of XXth International Archives of the Photogrammetry, Remote Sensing and Spatial Information Sciences, 35(Part B4)*, 12–23 July 2004, Istambul, Turkey (Istambul: ISPRS), pp. 1–6, (CD-ROM).

DAVIS, C.H. and WANG, X., 2003, Planimetric accuracy of Ikonos 1 m panchromatic orthoimage products and their utility for local government GIS basemap applications. *International Journal of Remote Sensing*, **24**, pp. 4267–4288.

EUR-LEX 2000, Council Regulation (EC) No. 1593/2000 of 17 July 2000 amending regulation (EEC) 3508/92 establishing an integrated administration and control system for certain Community aid schemes. Official Journal No. L 182, 21 July 2000, 4–7.

FRASER, C.S., 2002, Prospect for mapping from high-resolution satellite imagery. In *23rd Asian Conference on Remote Sensing (ACRS 2002)*, 25–29 November 2002, Kathmandu, Nepal (Kathmandu: ACRS), pp. 1–8 (CD-ROM).

FRASER, C.S. and HANLEY, H.B., 2005, Bias-compensated RPCs for sensor orientation of high-resolution satellite imagery. *Photogrammetric Engineering and Remote Sensing*, **71**, pp. 909–915.

FRASER, C.S. and YAMAKAWA, T., 2004, Insights into affine model for high-resolution satellite sensor orientation. *ISPRS Journal of Photogrammetry and Remote Sensing*, **58**, pp. 275–288.

FRASER, C.S., DIAL, G. and GRODECKI, J., 2006, Sensor orientation via RPCs. *ISPRS Journal of Photogrammetry and Remote Sensing*, **60**, pp. 182–194.

GRODECKI, J. and DIAL, G., 2003, Block adjustment of high-resolution satellite images described by rational polynomials. *Photogrammetric Engineering and Remote Sensing*, **69**, pp. 59–68.

HOLLAND, D.A., BOYD, D.S. and MARSHALL, P., 2006, Updating topographic mapping in Great Britain using imagery from high-resolution satellite sensors. *ISPRS Journal of Photogrammetry and Remote Sensing*, **60**, pp. 212–223.

KAY, S., 2002, *Implementation of IACS-GIS, Reg. 1593/00 and 2419/01*, MARS-PAC discussion documents, Joint Research Centre, Ispra, Italy. Available online at: http://mars.jrc.it/marspac/LPIS/default.htm (accessed 23 June 2006).

KAY, S., SPRUYT, P. and ALEXANDROU, K., 2003, Geometric quality assessment of orthorectified VHR space image data. *Photogrammetric Engineering and Remote Sensing*, **69**, pp. 484–491.

NIU, X., WANG, J., DI, K., LEE, J. and LI, R., 2004, Geometric modelling and photogrammetric processing of high-resolution satellite imagery. In *Proceedings of XXth International Archives of the Photogrammetry, Remote Sensing and Spatial Information Sciences, 35(Part B4)*, 12–23 July 2004, Istambul, Turkey (Istambul: ISPRS), pp. 1–6, (CD-ROM).

NOGUCHI, M., FRASER, C.S., NAKAMURA, T., SHIMONO, T. and OKI, S., 2004, Accuracy assessment of QuickBird stereo imagery. *Photogrammetric Record*, **19**, pp. 128–137.

RIDLEY, H., ATKINSON, P., APLIN, P., MULLER, J.P. and DOWMAN, I., 1997, Evaluating the potential of the forthcoming commercial U.S. high-resolution satellite sensor imagery at the Ordnance Survey. *Photogrammetric Engineering and Remote Sensing*, **63**, pp. 997–1005.

ROSSI, L. and VOLPE, F., 2005, Integrated cadastre system for EU agricultural subsidies. Italian response to the challenge of environmental sustainability. *GEOInformatics*, **8**, pp. 12–13.

SHAKER, A., SHI, W. and BARAKAT, H., 2005, Assessment of the rectification accuracy of IKONOS imagery based on two-dimensional models. *International Journal of Remote Sensing*, **26**, pp. 719–731.

TAO, C.V. and HU, Y., 2001, A comprehensive study of the rational function model for photogrammetric processing. *Photogrammetric Engineering and Remote Sensing*, **67**, pp. 1347–1357.

TAO, C.V., HU, Y. and JIANG, W., 2004, Photogrammetric exploitation of IKONOS imagery for mapping applications. *International Journal of Remote Sensing*, **25**, pp. 2833–2853.

TOUTIN, T., 2003, Error tracking in Ikonos geometric processing using a 3D parametric model. *Photogrammetric Engineering and Remote Sensing*, **69**, pp. 43–51.

TOUTIN, T., 2004, Review article: geometric processing of remote sensing images: models, algorithms and methods. *International Journal of Remote Sensing*, **25**, pp. 1893–1924.

TOUTIN, T., 2006, Comparison of 3D physical and empirical models for generating DSMs from stereo HR images. *Photogrammetric Engineering and Remote Sensing*, **72**, pp. 597–604.

TOUTIN, T. and CHENG, P., 2002, QuickBird – a milestone for high-resolution mapping. *Earth Observation Magazine*, **11**, pp. 14–18.

WANG, H. and ELLIS, E.C., 2005, Spatial accuracy of orthorectified IKONOS imagery and historical aerial photographs across five sites in China. *International Journal of Remote Sensing*, **26**, pp. 1893–1911.

WOLNIEWICZ, W., 2004, Assessment geometric accuracy of VHR satellite images. In *Proceedings of XXth International Archives of the Photogrammetry, Remote Sensing and Spatial Information Sciences, 35(Part B1)*, 12–23 July 2004, Istambul, Turkey (Istambul: ISPRS), pp. 1–5 (CD-ROM).

ZHOU, G. and LI, R., 2000, Accuracy evaluation of ground points from IKONOS high-resolution satellite imagery. *Photogrammetric Engineering and Remote Sensing*, **66**, pp. 1103–1112.